DOI: 10.1002/ejoc.201000778

(*R*)-(+)-[VCD(–)984]-4-Ethyl-4-methyloctane: A Cryptochiral Hydrocarbon with a Quaternary Chiral Center. (2) Vibrational CD Spectra of Both Enantiomers and Absolute Configurational Assignment

Shunsuke Kuwahara,[a,b] Kazuhiro Obata,[a] Takuma Fujita,[a] Nobuaki Miura,[c] Atsufumi Nakahashi,[c] Kenji Monde,[c] and Nobuyuki Harada*[a,d]

Keywords: Chirality / Optical rotation / Configuration determination / Density functional calculations / Conformational analysis / Vibrational spectroscopy

To characterize precisely the chiroptical properties of 4-ethyl-4-methyloctane (**1**), one of the so-called cryptochiral compounds, the enantiomer (*S*)-(–)-[VCD(+)984]-**1** was synthesized in an enantiopure form. The observed specific rotation values at 365 nm of both enantiomers agreed well, but were opposite in sign, confirming their enantiomeric relationship, although their absolute values were very small, reflecting their cryptochirality. The vibrational circular dichroism (VCD) spectra of both enantiomers were measured neat and showed characteristic Cotton effects around 1150–900 cm^{-1}; the VCD spectral curves were mirror images of each other. Based on the observed positive VCD band at 984 cm^{-1} for (*S*)-(–)-**1**, its absolute configuration was fully designated as (*S*)-(–)-[VCD(+)984]-**1**. The VCD spectrum was quantum chemically calculated by the DFT MO method at the B3PW91/6-31G(d,p) level, and the simulated VCD curve for (*S*)-**1** agreed very well with the observed VCD spectrum of (*S*)-(–)-**1**, confirming the absolute configuration.

Introduction

4-Ethyl-4-methyloctane (**1**), is the simplest saturated hydrocarbon with a quaternary chiral center to which four different unbranched alkyl groups, i.e., methyl, ethyl, propyl, and butyl groups, are bonded (Scheme 1). Hydrocarbon **1** is a so-called cryptochiral compound[1] because of its extremely small optical rotation, as reported in our short communication[2] and in Part 1 of this two-part paper.[3]

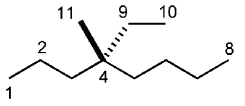

(*S*)-(–)-[VCD(+)984]-**1**

$[\alpha]_{365}{}^{21} = -0.73$ (neat, $\rho = 0.7565$)

Scheme 1. Absolute configuration of 4-ethyl-4-methyloctane {(*S*)-(–)-[VCD(+)984]-**1**} used in this study.

Chiral saturated hydrocarbon **1** has no UV chromophore and, therefore, it is silent for electronic circular dichroism (ECD) in the UV/Vis region. Hence, ECD spectroscopy is useless for characterization of alkane **1**. However, the vibrational circular dichroism (VCD, CD spectroscopy in the infrared region)[4–6] is applicable even to such compounds, because all compounds, including saturated hydrocarbons, naturally absorb IR light corresponding to vibrational excitation. VCD spectroscopy is thus suitable for the characterization of chiral compounds with no UV/Vis chromophore.

VCD spectroscopy has made remarkable progress in recent years.[4–6] The combination of many improvements in VCD spectrometers[7] and advances in quantum mechanical theories[8] has enabled the absolute configuration of most chiral organic compounds to be determined. Namely, application of the DFT MO method at the B3PW91/6-31G(d,p) level,[8] allows a VCD spectrum to be calculated that can be compared with the experimentally determined spectrum, leading to the assignment of absolute configurations. It is therefore intriguing to study how VCD is applicable to cryptochiral compounds such as alkane **1**, with very weak optical rotation.

We previously reported the VCD spectrum of 4-ethyl-4-methyloctane (*R*)-(+)-**1**,[2] for which the VCD intensity was ten-fold smaller than that of a standard compound, (1*R*)-(+)-α-pinene,[9] and thought that the small VCD intensity reflects the cryptochirality of hydrocarbon **1**. However, the signal-to-noise (S/N) ratio of the VCD spectrum was low and, therefore, it was prudent to measure the VCD spectra

---

[a] Institute of Multidisciplinary Research for Advanced Materials, Tohoku University,
2-1-1 Katahira, Aoba, Sendai 980-8577, Japan
E-mail: n2harada@tagen.tohoku.ac.jp
[b] Department of Chemistry, Toho University,
2-2-1 Miyama, Funabashi 274-8510, Japan
[c] Frontier Research Center for Post-Genome Science and Technology, Faculty of Advanced Life Science, Hokkaido University,
Kita 21 Nishi 11, Sapporo 001-0021, Japan
[d] Department of Chemistry, Columbia University,
3000 Broadway, New York, NY 10027, USA

of both enantiomers to check whether they were exactly mirror images or not. For this reason, we synthesized the other enantiomer (*S*)-(–)-**1**, the VCD spectrum of which was measured and compared with the theoretically calculated spectrum to determine the absolute configuration. In this Part 2 of a two-part paper, we report the details of the VCD spectroscopic studies of compound **1**.

Results and Discussion

Synthesis of Enantiopure 4-Ethyl-4-methyloctane [(*S*)-(–)-1]

The synthesis of the (*R*)-(+)-**1** enantiomer was reported in the Part 1 of this two-part paper.[3] According to the procedure described there, enantiopure 4-ethyl-4-methyloctane [(*S*)-(–)-**1**] was synthesized as shown in Scheme 2.

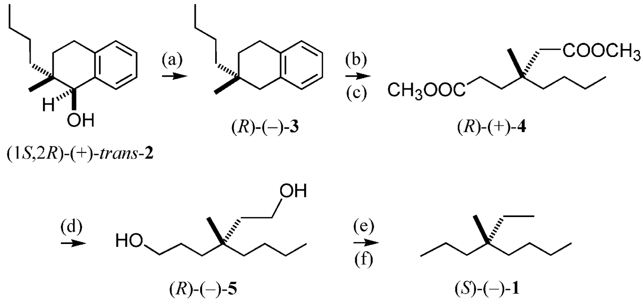

Scheme 2. Synthesis of enantiopure 4-ethyl-4-methyloctane [(*S*)-(–)-**1**]: (a) $NaBH_4$, $AlCl_3$, THF, reflux (81%). (b) $RuCl_3$, HIO_4, CCl_4, CH_3CN, H_2O. (c) MeI, K_2CO_3, DMF (51%). (d) $LiAlH_4$, THF (90%). (e) CBr_4, PPh_3, CH_2Cl_2. (f) $NaBH_4$, HMPA (71%).

Enantiopure *trans*-alcohol[2,3] (1*S*,2*R*)-(+)-**2** was reduced to yield 2-butyl-2-methyltetralin [(*R*)-(–)-**3**]. Oxidative cleavage of the benzene ring and successive esterification afforded diester (*R*)-(+)-**4**, which was then reduced to diol (*R*)-(–)-**5**. Finally, glycol (*R*)-(–)-**5** was converted into enantiopure 4-ethyl-4-methyloctane [(*S*)-(–)-**1**], the ^{13}C NMR spectrum of which was in complete agreement with those of (*R*)-(+)-**1** and (±)-**1**. To characterize the product, the specific rotation at the sodium D-line was first measured ($[\alpha]_D$ = –0.08), but the absolute value was almost half the value of (*R*)-(+)-**1** ($[\alpha]_D$ = +0.19) previously reported.[2] However, the absolute value ($[\alpha]_{365}$ = –0.73) at 365 nm agreed well with that of (*R*)-(+)-**1** ($[\alpha]_{365}$ = +0.70). It is thus advisable to use the larger optical rotation at shorter wavelength for such cryptochiral compounds. Namely, the optical rotation at 365 nm is useful for characterization of enantiomers of hydrocarbon **1**. For another chiroptical method, we next adopted VCD spectroscopy.

VCD Spectra of Both Enantiomers of 4-Ethyl-4-methyloctane (1)

The VCD spectrum of enantiopure hydrocarbon (*R*)-(+)-**1** was previously reported in a short communication,[2] where the spectrum was measured neat in a BaF_2 cell (cell length l = 46 μm, density ρ = 0.7565 g/cm^3, and acquisition time 3 h). The blank curve was obtained by using undecane, an achiral hydrocarbon with the same molecular formula, and the net VCD spectrum was obtained as [VCD(**1**) – VCD(blank)]. However, the S/N ratio of the observed spectrum was too poor to clearly characterize **1** by VCD spectroscopy. We had considered that the weak VCD spectrum and consequent poor S/N ratio might arise either from the cryptochirality of this hydrocarbon, or from the poor sensitivity of the VCD spectrometer used. To address this problem, it was important to measure the VCD spectrum of the other enantiomer (*S*)-(–)-**1** and to check whether the VCD spectra of both enantiomers were mirror images. To this end, the VCD spectrum of (*S*)-(–)-**1** was measured under the same conditions as indicated above, except for the cell length (l = 45 μm). In addition, the VCD blank curve was obtained by using racemic hydrocarbon (±)-**1**, the preparation of which was reported in our short communication[2] and Part 1 of this two-part paper.[3]

The VCD spectrum of (*S*)-(–)-**1** from 1350 to 900 cm^{-1} is shown in Figure 1 (b), together with the IR spectrum and the VCD blank curve, in which the VCD spectra were corrected against the standard *A*-value of (1*R*)-(+)-α-pinene,[9] as described in the Experimental Section. It can be seen that the S/N ratio was much improved this time, as judged from the VCD blank curve [Figure 1 (c)]. In addition, the VCD curve is almost flat in the region from 1350 to 1150 cm^{-1}. It should be noted that the VCD spectrum clearly shows characteristic, intense, positive and negative bands in the so-called fingerprint region ranging from 1150 to 900 cm^{-1}, whereas the IR spectrum shows weak and broad bands in this region [Figure 1 (a)]. Because a positive VCD band was observed at 984 cm^{-1} ($\Delta\varepsilon = +3.2 \times 10^{-3}$), the (*S*) enantiomer was designated as (*S*)-[VCD(+)984]-**1**, which means that the enantiomer showing a positive VCD at 984 cm^{-1} has the (*S*) absolute configuration.

In our previous short communication,[2] we used the VCD band at 945 cm^{-1} for the designation of enantiomer **1**, but later it was suggested that the use of the VCD band at 984 cm^{-1} is more general because of the larger VCD intensity at the latter frequency. Therefore, the (*R*)-enantiomer previously reported[2] is now designated as (*R*)-(+)-[VCD(–)984]-**1** {= (*R*)-(+)-[VCD(+)945]-**1**}. It should be noted that this is just a change of designation of enantiomer, not a change of absolute configurational assignment.

It was found that the VCD spectrum of (*S*)-(–)-[VCD(+)984]-**1** is much stronger than that of (*R*)-(+)-[VCD(–)984]-**1** previously reported[2] and, therefore, the VCD spectrum of (*R*)-**1** was corrected against the standard *A*-value of (1*R*)-(+)-α-pinene. After the correction, both VCD spectra were found to be mirror images, as seen in the region from 1150 to 900 cm^{-1} [Figure 2 (a)], i.e., the corresponding VCD bands are opposite in sign to each other, but similar in intensity. From these results, it is unambiguously concluded that the VCD bands between 1150 and 900 cm^{-1} clearly reflect the chirality of both enantiomers, and are therefore useful as chiroptical markers for characterization. Thus, it is an advantage to measure the VCD spectra of

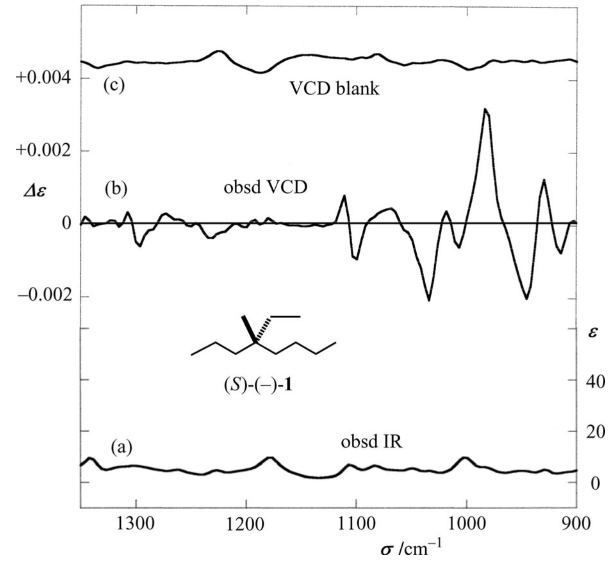

Figure 1. VCD and IR spectra of 4-ethyl-4-methyloctane {(*S*)-(–)-[VCD(+)984]-**1**}: (a) IR spectrum measured neat; (b) VCD spectrum measured neat; (c) VCD blank measured neat by using racemic 4-ethyl-4-methyloctane.

both enantiomers, and it is advisable to correct the VCD data against the *A*-value of a standard sample, (1*R*)-(+)-α-pinene.[9]

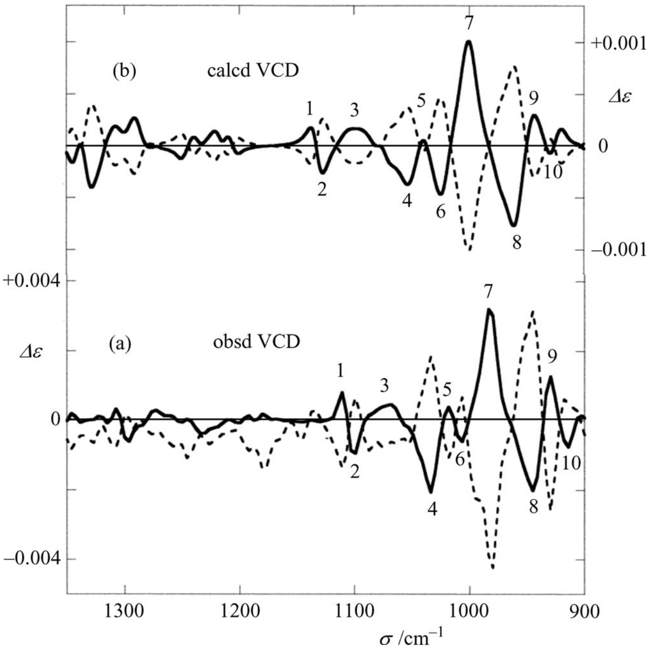

Figure 2. Observed and calculated VCD spectra of 4-ethyl-4-methyloctane enantiomers: (a) Observed VCD spectrum of (*S*)-(–)-[VCD(+)984]-**1** (solid line) and observed VCD of (*R*)-(+)-[VCD(–)984]-**1** (dotted line); (b) calculated VCD spectrum of (*S*)-**1** (solid line) and calculated VCD of (*R*)-**1** (dotted line). The numbers indicated on the solid lines specify VCD Cotton effects and show the one-to-one correspondence between experimental and theoretical VCD bands.

Calculation of the VCD Spectra of 4-Ethyl-4-methyloctane by the DFT MO Method and Determination of the Absolute Configuration by Comparison of Experimental and Theoretical VCD Spectra

In recent years, there have been many advances in the ab initio calculation of VCD spectra,[8] which has enabled the absolute configuration of a target compound to be determined by comparison of the experimental and theoretical VCD spectra. Thus, the VCD spectrum of 4-ethyl-4-methyloctane (*R*)-**1** was calculated as follows:[10] (i) the stable conformers of (*R*)-**1** were searched by the CONFLEX method using the MMFF94S force field, giving 30 conformers, the Boltzmann populations of which were summed to exceed 95%; (ii) the structure–energy minimization of conformers and harmonic oscillation analysis were carried out by the DFT MO method at the B3PW91/6-31G(d,p) level[8] and, after calculating the vibrational entropy and correcting for free energy at 298.15 K, the relative stability of each conformer was evaluated based on the free energy; (iii) based on the relative free energies, stable conformers were selected until the sum of the Boltzmann population exceeded 95%, leading to the 24 stable conformers listed in Table 1; (iv) the VCD and IR spectra of each conformer were calculated by the DFT method, where the spectral band was approximated by the Lorentzian equation, and the parameter γ, half the bandwidth at half peak height, was used as $\gamma = 8\ \text{cm}^{-1}$. The total averaged VCD and IR spectra were then simulated by using the Boltzmann weighting.

Among the 24 stable conformers of (*R*)-**1**, five major conformers with large population are illustrated in Figure 3. The most stable conformer, #02 (14.7% population) has a stereostructure in which the octane moiety containing the propyl and butyl groups takes a linear and all-*trans* conformation, and the butane moiety, containing the methyl and ethyl groups, also takes a linear and all-*trans* conformation. Both moieties are perpendicular to each other as shown.

A similar all-*trans* conformation is seen in the second most stable conformer #01 (10.9% population); in this case, the heptane moiety containing the ethyl and butyl groups also takes a linear and all-*trans* conformation, and the pentane moiety containing the methyl and propyl groups are also linear and all-*trans*. These two moieties are perpendicular to each other. The third most stable conformer #00 (7.9% population) also takes a similar all-*trans* conformation, where the hexane moiety, which is composed of ethyl and propyl groups, is linear and all-*trans*, and the second hexane moiety, containing methyl and butyl groups, is also linear and all-*trans*. The two moieties are perpendicular to each other. These linear and all-*trans* conformations are characteristic features of these three stable conformers.

The fourth stable conformer #13 (5.5% population) has a different conformation from those of the previous stable conformers. Namely, the octane moiety containing the propyl and butyl groups has a *gauche* conformation in the propyl group [Figure 3 (d)]. A similar *gauche* conformation is also seen in the ethyl group. The conformer #13 thus has

Table 1. Calculated conformers of 4-ethyl-4-methyloctane (*R*)-**1** and their VCD rotational strength data around 1000 and 960 cm^{-1}.

Entry	Conformer	Relative free energy[a] ΔG [kcal mol^{-1}]	Population [%][b]	VCD(1000)[c] $R \times 10^{44}/\sigma_{ext}$ [cm^{-1}]	VCD(960)[d] $R \times 10^{44}/\sigma_{ext}$ [cm^{-1}]
1	#02	0.000	14.72	–3.88/1015.2	**+14.38/959.1**[e]
2	#01	0.181	10.85	–1.37/1005.8	**+11.24/973.7**[e]
3	#00	0.366	7.93	**–25.40/999.8**[e]	–1.94/956.3
4	#13	0.584	5.49	**–16.75/1003.3**[e]	–3.99/962.7
5	#04	0.589	5.44	**–18.66/999.2**[e]	+5.43/956.9
6	#08	0.594	5.40	+3.12/1014.4	+7.39/961.7
7	#11	0.607	5.28	–3.60/1006.8	+6.51/962.0
8	#03	0.629	5.08	–9.46/1001.9	–7.90/972.7
9	#07	0.636	5.03	+2.75/1008.4	+12.44/966.3
10	#05	0.667	4.77	–18.20/1004.7	+8.58/956.7
11	#06	0.790	3.88	+15.13/1016.7	–5.90/962.0
12	#28	1.027	2.60	+2.61/ 998.7	–0.13/962.5
13	#16	1.155	2.09	+0.19/1003.6	+31.23/962.0
14	#12	1.199	1.94	+0.18/997.9	+15.41/972.3
15	#10	1.209	1.91	–23.14/995.8	+1.21/959.0
16	#09	1.244	1.80	–26.87/998.2	+7.58/959.4
17	#20	1.265	1.74	+1.32/ 999.3	+7.06/963.2
18	#14	1.295	1.65	+0.31/995.7	+17.72/971.8
19	#25	1.360	1.48	+2.70/998.2	+13.35/961.7
20	#15	1.368	1.46	–15.08/994.1	+0.68/972.3
21	#23	1.421	1.34	–10.74/997.8	+7.52/958.3
22	#19	1.431	1.31	+1.11/1002.8	+10.23/961.5
23	#27	1.439	1.29	+11.70/1000.5	+15.38/962.0
24	#21	1.532	1.11	–16.95/999.3	+7.78/959.7

[a] Relative free energy at 298.15 K. [b] Total population 1–24 = 95.59 % [c] Calculated VCD rotational strength (*R* in cgs units) and transition wavenumber (σ_{ext}) around 1000 cm^{-1}. [d] Calculated VCD rotational strength (*R* in cgs units) and transition wavenumber (σ_{ext}) around 960 cm^{-1}. [e] Major VCD data.

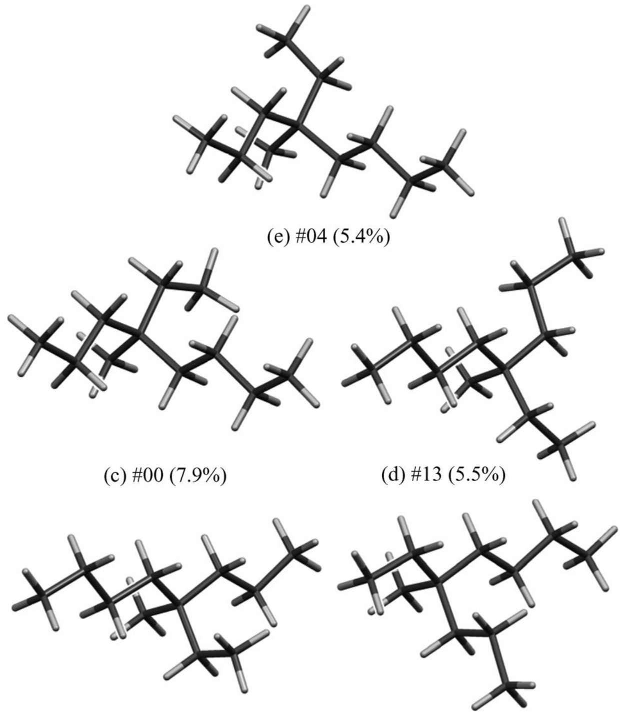
(e) #04 (5.4%)

(c) #00 (7.9%)

(d) #13 (5.5%)

(a) #02 (14.7%)

(b) #01 (10.9%)

Figure 3. Five major conformers of 4-ethyl-4-methyloctane (*R*)-**1** obtained by the DFT method at the B3PW91/6-31G(d,p) level.

two *gauche* moieties, taking a higher energy. The fifth stable conformer #04 (5.4 % population) also has a *gauche* moiety. Namely, the hexane moiety containing the ethyl and propyl groups takes a *gauche* conformation in the ethyl group, whereas the hexane moiety containing methyl and butyl groups is linear and all-*trans* in conformation.

The IR spectrum of 4-ethyl-4-methyloctane (**1**) was then calculated by using the DFT MO method at the B3PW91/6-31G(d,p) level as shown in Figure 4; the numbered peaks show the excellent one-to-one correspondence between experimental and theoretical IR spectra, although the calculated IR band is shifted to a higher wavenumber than the observed band. The IR band 1 was assigned to the CH_2 bending and CH_3 asymmetric bending vibrations, whereas band 2 was due to the CH_3 symmetric bending vibration. It is thus noteworthy that the experimental and theoretical IR curves agree well, which indicates the reliability of the DFT MO method used here.

To determine the absolute configuration of 4-ethyl-4-methyloctane (**1**), the VCD spectra of the 24 most stable conformers listed in Table 1 were calculated by the DFT MO method at the B3PW91/6-31G(d,p) level. Among the VCD data obtained, the rotational strengths (*R*) around 1000 and 960 cm^{-1} are listed in Table 1. The total theoretical VCD spectrum of 4-ethyl-4-methyloctane (*R*)-**1** was then calculated based on the Boltzmann weighting, which is shown by the dotted line in Figure 2 (b); the theoretical VCD spectrum of the other enantiomer (*S*)-**1** is also shown (solid line) for comparison with the experimental spectrum.

It should be emphasized that the experimental and theoretical VCD spectra of (*S*)-**1** are in good agreement [solid lines in Figure 2 (a) and (b)]. Especially the VCD spectra in the region from 1150 to 900 cm^{-1} show an excellent one-to-one correlation between experimental and theoretical VCD

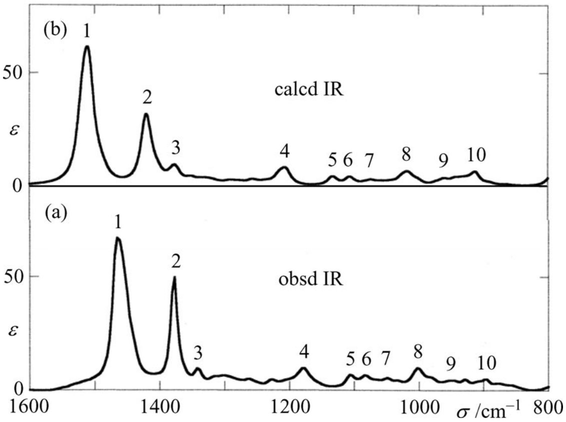

Figure 4. Observed and calculated IR spectra of 4-ethyl-4-methyloctane **1**: (a) observed; (b) calculated. The values specify IR peaks and shows the one-to-one correspondence between experimental and theoretical IR bands.

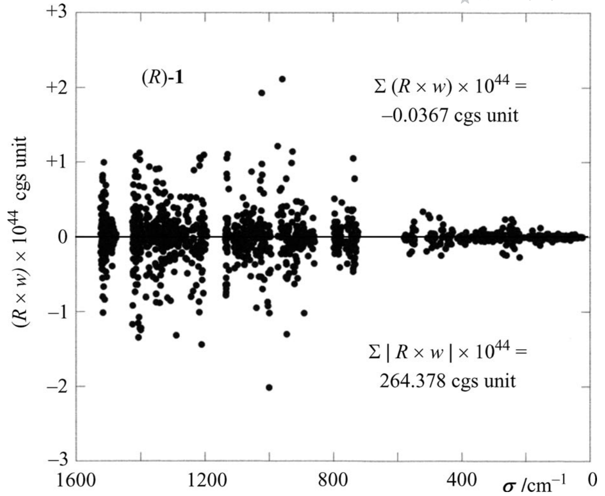

Figure 5. Boltzmann-weighted rotational strength ($R \times w$) in cgs units calculated for all transitions in the 24 most stable conformers of (*R*)-**1** in the range 1600–0 cm^{-1}.

bands [compare the numbered VCD bands in Figure 2 (a) and (b)]. For example, the strongest positive VCD band (#7) calculated at 1001 cm^{-1} corresponds to the strongest positive VCD band (#7) observed at 984 cm^{-1}, whereas the second strongest negative band (#8) calculated at 961 cm^{-1} corresponds to the intense negative band (#8) observed at 945 cm^{-1}. Other observed VCD bands designated as #1–#6 and #9–#10 were also reproduced well by the DFT MO calculation, as seen in Figure 2.

The experimental and theoretical VCD spectra of chiral hydrocarbon **1** are thus in complete agreement and, as a consequence, the absolute configuration of compound [VCD(+)984]-**1** was unambiguously determined to be *S*, which is consistent with the previous determination by X-ray crystallographic analysis and chemical correlation described in Part 1 of this two-part paper.[3]

Analysis of the VCD Transitions and Vibrational Mode

To gain insight into the VCD generation mechanism of hydrocarbon **1**, the composition of the VCD bands was analyzed as follows. Figure 5 shows the products ($R \times w$) of rotational strength (R) and Boltzmann weight (w) calculated for all transitions in the 24 stable conformers of (*R*)-**1** in the range 1600–0 cm^{-1} as dots. The data points are much condensed near the zero line, where each conformer has 75 vibrational transitions. At first glance, the distribution looks almost symmetrical along the zero line, which indicates that the sum rule ($\Sigma R = 0$) holds also for the VCD spectra. The summation [$\Sigma(R \times w)$] was calculated for all transitions from 1600 to 0 cm^{-1}, giving $\Sigma(R \times w) = -0.0367 \times 10^{-44}$ cgs units, which is very much smaller than the summation of the absolute values $\Sigma|R \times w| = 264.378 \times 10^{-44}$ cgs units. Namely, the sum rule holds approximately in this case.

In such a symmetrical distribution of the Boltzmann-weighted rotational strength, the positive data points cancel out the negative points, and hence the resultant VCD becomes almost zero or very weak. The VCD spectrum is thus sensitive to the rotational strength and population of conformers.

As discussed above, the VCD spectrum around 1150–900 cm^{-1} was excellently reproduced by the DFT calculation. Therefore, this region was expanded in Figure 6, where the calculated VCD curve is also illustrated. In the region around 1130 cm^{-1}, the distribution still looks symmetrical. However, on closer examination, the negative data points are located at higher wavenumbers than the positive points, generating a negative VCD at higher wavenumbers and a positive VCD at lower wavenumbers. The assignment of the VCD bands in this region thus becomes clearer.

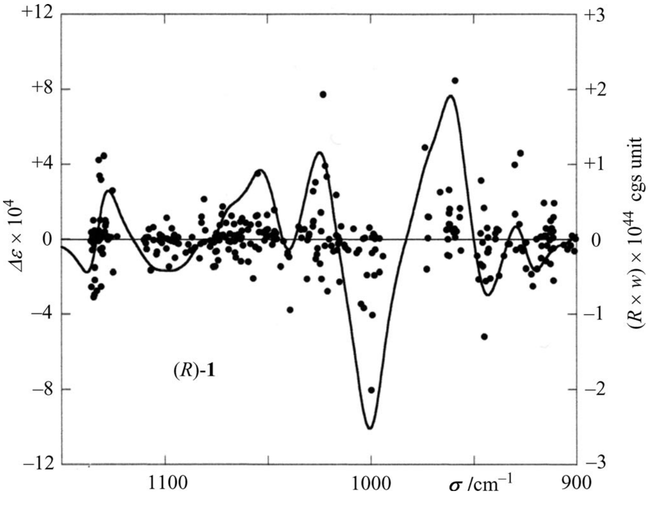

Figure 6. Calculated Boltzmann-weighted rotational strength and VCD for (*R*)-**1** in the range 1150–900 cm^{-1}: Dots show the product ($R \times w$) in cgs units for all transitions in the 24 most stable conformers; the calculated VCD spectrum is shown as a solid line.

It is interesting that a composition of the intense VCD bands at 1000 and 960 cm^{-1} is much more simple and clear. Namely, in the region around 1000 cm^{-1}, most of the data points cluster on the negative side, generating the strongest negative VCD band (Figure 6). The rotational strength (*R*) data of the VCD transitions around this frequency are also listed in Table 1, where most conformers have negative *R* values, especially conformers #00, #13, and #04, which make dominant contributions. On the other hand, in the region around 960 cm^{-1}, most data points are found on the positive side, making the second strong positive VCD; especially conformers #02 and #01 with large *R* values that dominantly contribute to the positive VCD (Table 1). The composition of the two bands is thus simple, which makes the assignment much more reliable for the determination of the absolute configuration of cryptochiral hydrocarbon **1**.

To gain further insight into the VCD mechanism, the vibrational mode of the transitions responsible for the VCD around 1000 or 960 cm^{-1} in the five most stable conformers was investigated (Figure 7). For example, in the most stable conformer #02, the transition generating the positive VCD at 959 cm^{-1} has the vibrational mode shown in Figure 7 (a), where most protons make an out-of-plane C–H bending motion. The protons in the methyl and propyl groups show especially large motions. In another conformer, #01, which displays a positive VCD shoulder around 974 cm^{-1}, C–H bending in the methyl and propyl groups make large contributions, whereas most protons in the butyl group do not [Figure 7 (b)].

The vibrational modes of the transitions responsible for the negative VCD around 1000 cm^{-1} in the remaining three major conformers are illustrated in Figure 7 (c–e). In conformer #00, the protons in the ethyl and propyl groups show large C–H bending, while those of the butyl group displayed no motion. In conformer #13, the protons of the methyl, ethyl, and propyl groups make a C–H bending motion, whereas those of the butyl group again showed no motion. In the case of conformer #04, the protons of the ethyl and propyl groups make a large contribution, whereas those of the butyl group again do not. There are thus some

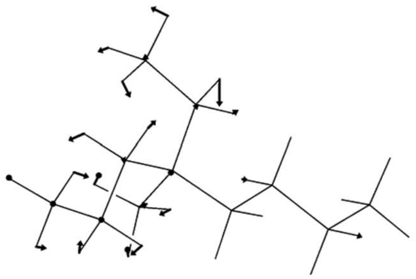

(e) #04 VCD(–)/999 cm^{-1}

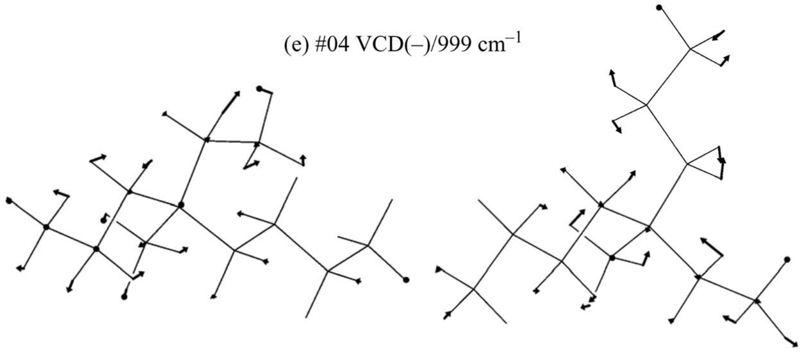

(c) #00 VCD(–)/1000 cm^{-1} (d) #13 VCD(–)/1003 cm^{-1}

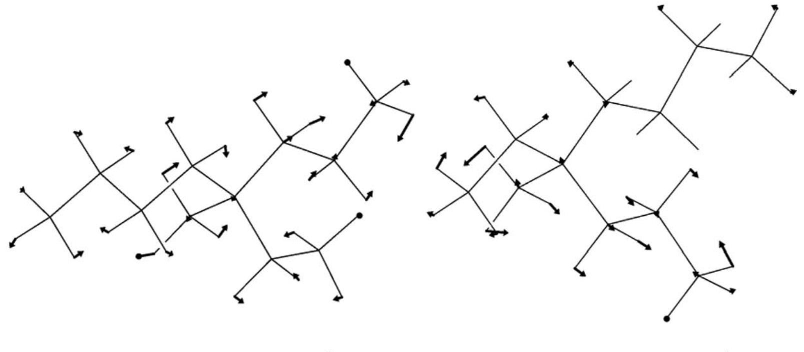

(a) #02 VCD(+)/959 cm^{-1} (b) #01 VCD(+)/974 cm^{-1}

Figure 7. Vibrational modes of the transitions responsible for the VCD around 1000 or 960 cm^{-1} in the five most stable conformers of (*R*)-**1**.

similarities in the vibrational modes (c)–(e). However, it was difficult to rationalize these modes and to correlate them with the negative VCD in a qualitative sense.

Conclusions

The enantiopure chiral hydrocarbon, (*S*)-(–)-4-ethyl-4-methyloctane (**1**), was synthesized, and its VCD spectrum was measured with a high S/N ratio. The VCD and IR spectra of hydrocarbon **1** were calculated by the DFT MO method at the B3PW91/6-31G(d,p) level, and the calculated IR curve agreed well with the observed spectrum. The VCD curve obtained for (*S*)-**1** agreed very well with the observed spectrum of the [VCD(+)984] enantiomer, especially in the 1150–900 cm^{-1} region, which confirmed the absolute configuration of **1** previously determined by X-ray crystallographic analysis and by ^{1}H NMR anisotropy. The VCD bands in the 1150–900 cm^{-1} region were studied by analyzing the Boltzmann-weighted rotational strength and vibrational modes, which made the absolute configurational assignment more reliable. The absolute configuration of (*S*)-(–)-[VCD(+)984]-**1** was thus established.

Experimental Section

General Methods: IR spectra were obtained as neat, film on KBr, or KBr disks with a Jasco FT/IR-410 spectrophotometer. ^{1}H NMR spectra were recorded with a Jeol JNM-LA400 (400 MHz) and/or a Jeol JNM-LA600 (600 MHz) spectrometer. ^{13}C NMR spectra were obtained with a Jeol JNM-LA400 (100 MHz), a Jeol JNM-ECP400 (100 MHz), and/or a Jeol JNM-LA600 (150 MHz) spectrometer. All NMR spectroscopic data for $CDCl_3$ and CD_2Cl_2 solutions are reported in ppm (δ) downfield from TMS. Optical rotations $[\alpha]_{\mathrm{D}}$ were measured with a Jasco DIP-1000 spectropolarimeter. Silica gel 60 F_{254} precoated plates on glass from Merck Ltd. were used for thin layer chromatography (TLC). HPLC separation and purification were performed by using a prepacked glass column (22 × 300 mm, or 25 × 400 mm) of silica gel (particle size 5–10 µm) from Kusano Co. Ltd. and a UV/RI detector (Shimamura YRU-880). The purities of the title compounds were shown to be ≥99% by ^{1}H NMR, TLC, HPLC, and/or elemental analyses.

Measurement of VCD and IR Spectra: The VCD and IR spectra of enantiopure compounds were measured from 400 to 4000 cm^{-1} by using a ChiralIR VCD spectrometer from BioTools Inc. under the following conditions: resolution 3.9 cm^{-1}; BaF_2 cell (International Crystal Laboratories Inc.), cell length l = 45 µm or 46 µm; neat, density ρ = 0.7565 g/cm^3; acquisition time: 3 h. The net VCD spectra were obtained as [VCD(sample) – VCD(blank)], where the racemic sample or a closely related achiral compound was used as the blank sample. The net IR spectra were obtained as [IR(sample) – IR(cell)].

Calibration of VCD Scale: Calibration was carried out by using (1*R*)-(+)-α-pinene as the standard sample as follows. The VCD $\Delta\varepsilon$ values of (1*R*)-(+)-α-pinene were reported by L. A. Nafie and coworkers.[9] Among the data, the two intense bands at 1124 cm^{-1} ($\Delta\varepsilon = +1.0 \times 10^{-2}$) and 1101 cm^{-1} ($\Delta\varepsilon = -8.4 \times 10^{-3}$) were selected as standard values of the amplitude, A-value = $\Delta\varepsilon$(1124 cm^{-1}) – $\Delta\varepsilon$(1101 cm^{-1}) = $+1.84 \times 10^{-2}$. The intensity of the VCD spectra was corrected against this A-value of (1*R*)-(+)-α-pinene: neat, density ρ = 0.857 g/cm^3.

Preparation of Enantiopure 2-Butyl-2-methyltetralin (*R*)-(–)-3: A mixture of alcohol (1*S*,2*R*)-(+)-*trans*-**2** (0.486 g, 2.23 mmol), $NaBH_4$ (0.421 g, 11.1 mmol), anhydrous $AlCl_3$ (1.34 g, 10.0 mmol), and THF (23 mL) was stirred at 80 °C for 15 h. The reaction was quenched with aqueous NH_4Cl at 0 °C, and the THF solvent was evaporated under reduced pressure. The mixture was extracted with EtOAc, and the organic layer was washed with brine, dried with anhydrous $MgSO_4$, and the solvents were evaporated to dryness. The crude product was purified by short column chromatography on silica gel (hexane/EtOAc, 50:1) and reverse-phase HPLC by using a ODS column (MeOH) yielding (*R*)-(–)-2-butyl-2-methyltetralin (**3**; 0.363 g, 81%) as a colorless oil. $[\alpha]_{\mathrm{D}}^{23} = -2.3$ (c = 1.87, $CHCl_3$). $[\alpha]_{\mathrm{D}}^{26} = -1.8$ (c = 2.21, cyclohexane). IR, ^{1}H NMR, and ^{13}C NMR spectroscopic data were identical with those of (*S*)-(+)-**3** reported in Part 1 of thistwo-part paper.[3] $C_{15}H_{22}$ (202.34): calcd. C 89.04, H 10.96; found C 88.96, H 11.26.

Preparation of Enantiopure Dimethyl 3-Butyl-3-methyladipate (*R*)-(+)-4: 2-Butyl-2-methyltetralin (*R*)-(–)-**3** (0.632 g) was treated as described for the opposite enantiomer,[3] yielding (*R*)-(+)-**4** (0.392 g, 51%) as a colorless oil. $[\alpha]_{\mathrm{D}}^{23} = +1.2$ (c = 1.89, $CHCl_3$). IR, ^{1}H NMR, and ^{13}C NMR spectroscopic data were identical with those of (*S*)-(–)-**4**.[3]

Preparation of Enantiopure 3-Butyl-3-methyl-1,6-hexanediol (*R*)-(–)-5: Dimethyl 3-butyl-3-methyladipate (*R*)-(+)-**4** (0.330 g) was treated as described for the opposite enantiomer,[3] yielding (*R*)-(–)-**5** (0.229 g, 90%) as a colorless oil. $[\alpha]_{\mathrm{D}}^{24} = -0.83$ (c = 2.27, $CHCl_3$). IR, ^{1}H NMR, and ^{13}C NMR spectroscopic data were identical with those of (*S*)-(+)-**5**.[3]

Preparation of Enantiopure 4-Ethyl-4-methyloctane (*S*)-(–)-1: 3-Butyl-3-methyl-1,6-hexanediol (*R*)-(–)-**5** (0.158 g) was treated as described for the opposite enantiomer,[3] yielding (*S*)-(–)-**1** (0.094 g, 71%) as a colorless oil. $[\alpha]_{365}^{21} = -0.73$ (neat, ρ = 0.7565). ^{13}C NMR (100 MHz, CD_2Cl_2): δ = 8.10 (C-10), 14.35 (C-8), 15.25 (C-1), 17.04 (C-2), 24.11 (C-7), 24.69 (C-11), 26.11 (C-6), 31.89 (C-9), 35.14 (C-4), 38.99 (C-5), 41.89 (C-3) ppm. IR and ^{1}H NMR spectroscopic data were identical with those of (*R*)-(+)-**1**.[3] HRMS: m/z calcd. for $C_{11}H_{24}$ $[M]^+$ 156.1878; found 156.1872.

Acknowledgments

The authors thank Dr. George A. Ellestad and Prof. Koji Nakanishi, Department of Chemistry, Columbia University, and Prof. Laurence A. Nafie, Department of Chemistry, Syracuse University, for their valuable suggestions. This work was supported in part by grants from the Japan Society for Promotion of Science Scientific Research (to N. H.), the Nissan Science Foundation (to S. K.), the Mazda Foundation (to S. K.), and the Inamori Foundation (to S. K.), and grant-in aids for scientific research from the Ministry of Education, Science, Sports, and Culture of Japan (Grants 20310127, 20651055). A. N. gratefully acknowledges a fellowship from the Japan Society of the Promotion of Science.

---

[1] K. Mislow, P. Bickart, *Isr. J. Chem.* **1976–1977**, *15*, 1–6; K. Mislow, *Collect. Czech. Chem. Commun.* **2003**, *68*, 849–864.

[2] T. Fujita, K. Obata, S. Kuwahara, N. Miura, A. Nakahashi, K. Monde, J. Decatur, N. Harada, *Tetrahedron Lett.* **2007**, *48*, 4219–4222.

[3] T. Fujita, K. Obata, S. Kuwahara, A. Nakahashi, K. Monde, J. Decatur, N. Harada, *Eur. J. Org. Chem.*, DOI: 10.1002/ejoc.201000777.

[4] a) R. K. Dukor, L. A. Nafie, in *Encyclopedia of Analytical Chemistry* (Ed.: R. A. Meyers), John Wiley & Sons, Hoboken,

New Jersey, **2000**, pp. 662–676; b) L. A. Nafie, *Chirality* **2003**, *15*, 743–758.

[5] P. L. Polavarapu, J. He, *Anal. Chem.* **2004**, *76*, 61A–67A.

[6] a) T. Taniguchi, N. Miura, S. Nishimura, K. Monde, *Mol. Nutr. Food Res.* **2004**, *48*, 246–254; b) T. Taniguchi, K. Monde, *Trends Glycosci. Glycotech.* **2007**, *19*, 147–164.

[7] For advanced VCD spectrometers, visit http://btools.com, http://www.jascoinc.com/, and http://www.brukeroptics.com/.

[8] M. J. Frisch, G. W. Trucks, H. B. Schlegel, G. E. Scuseria, M. A. Robb, J. R. Cheeseman, J. A. Montgomery, T. Vreven, K. N. Kudin, J. C. Burant, J. M. Millam, S. S. Iyengar, J. Tomasi, V. Barone, B. Mennucci, M. Cossi, G. Scalmani, N. Rega, G. A. Petersson, H. Nakatsuji, M. Hada, M. Ehara, K. Toyota, R. Fukuda, J. Hasegawa, M. Ishida, T. Nakajima, Y. Honda, O. Kitao, H. Nakai, M. Klene, X. Li, J. E. Knox, H. P. Hratchian, J. B. Cross, C. Adamo, J. Jaramillo, R. Gomperts, R. E. Stratmann, O. Yazyev, A. J. Austin, R. Cammi, C. Pomelli, J. W. Ochterski, P. Y. Ayala, K. Morokuma, G. A. Voth, P. Salvador, J. J. Dannenberg, V. G. Zakrzewski, S. Dapprich, A. D. Daniels, M. C. Strain, O. Farkas, D. K. Malick, A. D. Rabuck, K. Raghavachari, J. B. Foresman, J. V. Ortiz, Q. Cui, A. G. Baboul, S. Clifford, J. Cioslowski, B. B. Stefanov, G. Liu, A. Liashenko, P. Piskorz, I. Komaromi, R. L. Martin, D. J. Fox, T. Keith, M. A. Al-Laham, C. Y. Peng, A. Nanayakkara, M. Challacombe, P. M. W. Gill, B. Johnson, W. Chen, M. W. Wong, C. Gonzalez, J. A. Pople, *Gaussian 03*, Revision C.02, Gaussian, Inc., Wallingford, CT, **2004**.

[9] C. Guo, R. D. Shah, R. K. Dukor, T. B. Freedman, X. Cao, L. A. Nafie, *Vib. Spectrosc.* **2006**, *42*, 254–272.

[10] Recently, a TDDFT calculation for the optical rotation of chiral hydrocarbon **1** was reported, see: S. Grimme, C. Muck-Lichtenfeld, *Chirality* **2008**, *20*, 1009–1015.

Received: May 30, 2010